Sensitivity analysis of erosion on the landward slope of an earthen flood defence located in southern France submitted to wave overtopping

Clément Lutringer[1,2], Adrien Poupardin[1], Philippe Sergent[3], Abdelkrim Bennabi[1], and Jena Jeong[1,2]

[1]ESTP Paris, 28 Avenue du Président Wilson, 94230 Cachan, France
[2]Gustave Eiffel University, Cité Descartes, 77200 Marne-la-Vallée, France
[3]CEREMA Risques Eau Mer, 134 rue de Beauvais, 60280 Margny-les-Compiègne, France

Correspondence: Clément Lutringer (clutringer@estp-paris.eu)

Abstract. The study aims to provide a complete analysis framework applied to an earthen dyke located in Camargue, France. This dyke is regularly submitted to erosion on the landward slope that needs to be repaired. Improving the resilience of the dyke calls for a reliable model of damage frequency. The developed system is a combination of copula theory, empirical wave propagation, and overtopping equations as well as a global sensitivity analysis in order to provide the return period of erosion damage on a set dyke while also providing recommendations in order for the dyke to be reinforced as well the model to be self-improved. The global sensitivity analysis requires to calculate a high amount of return periods over random observations of the tested parameters. This gives a distribution of the return periods, providing a more general approach to the behavior of the dyke. The results show a return period peak around the two-year mark, close to reported observation. The distribution being skewed, the mean value is however higher and is thus less reliable as a measure of dyke safety. The results of the global sensitivity analysis show that no particular category of dyke features contribute significantly more to the uncertainty of the system. The highest contributing factors are the dyke height, the critical velocity as well as the coefficient of seaward slope roughness. These results underline the importance of good dyke characterization in order to improve the predictability of return periods estimations. The obtained return periods have been confirmed by current *in situ* observations but the uncertainty increases for the most severe events due to the lack of long-term data.

1 Introduction

The site of the Salin-de-Giraud located in the Camargue area in southern France is a historically low-lying region and is thus frequently exposed to numerous storms. The latest Intergovernmental Panel on Climate Change report (Pörtner et al., 2022) points to a general increase in the variability of extreme events. Storm surges are expected to become more violent and the climate generally more uncertain, meaning that correctly designing structures to withstand rare events is becoming more difficult than ever. In fact, all the infrastructures on the site as well as the land itself must be maintained in order to ensure its exploitation and new methods must be applied in order to keep the maintenance cost at a reasonable level. An earthen dyke, named Quenin, has been constructed on the site in order to protect the salt marshes during storm surges. The structure is quite

large, covering a few kilometers along the coastline. The dyke is approximately 2 meters high with large rocks on the seaward slope while the landward slope is only covered by sand (fig. 1-b).
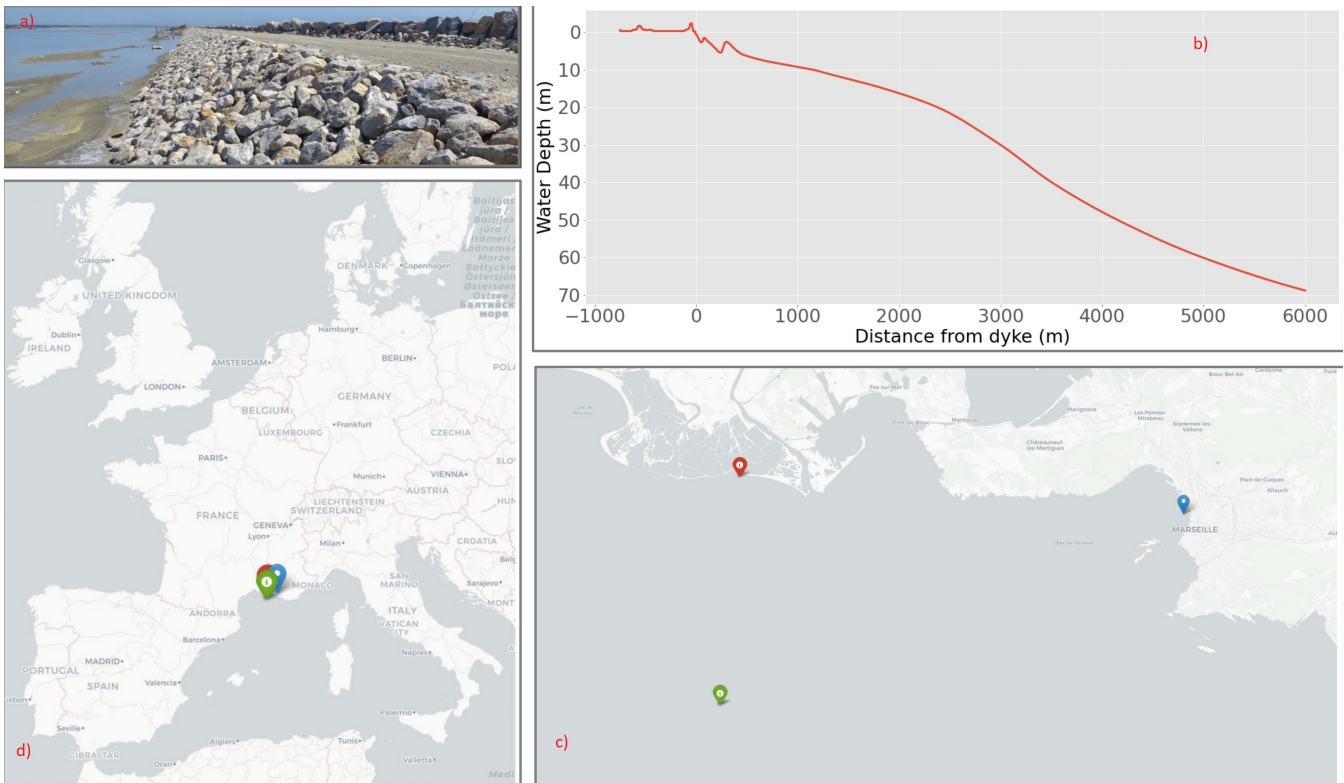
Figure 1. (a) Picture of the landward slope of the dyke, made of sand and clay. (b) Water Depth of the beach in front of the dyke with resolution $\Delta x = 3m$. (c) Regional map of Western Europe with the location of the dyke (red), deepwater wave gauge (green) and sea level records (blue). (d) Regional location of the data sources.

25   The erosion problem of the dyke is common in this area and therefore assessment of erosion is necessary. The semi-empirical approach based on hydraulic loading has been well-established and traditionally used. Wave propagation from deep water to the surf-zone has been well explored both analytically, numerically, and experimentally in the literature. A large overview of the theory surrounding random sea wave propagation theory was provided by Goda (2000) and brought advice on coastal protection. An evaluation of the different available methods on the subject has also been given by Liu and Han (2017). The

30   complex nature of the overtopping phenomena makes it more difficult to model using only simple equations. Thus many large-scale experiments have been conducted to deduce empirical laws as done by van der Meer (2011) as well as Hughes and Nadal (2008); Hughes et al. (2012) with the use of the Wave Overtopping Simulator. Numerical simulations have also been explored by Li et al. (2003) using the Volume of Fluid method. More recently, the EurOtop manual (van der Meer et al., 2018) laid an extensive set of recommendations and experimentally based equations in order to functionally model the overtopping

35   phenomenon. Bergeijk et al. (2019) also provided a more refined analytical model of overtopping using a set of coupled

equations validated by numerical simulations and experiments.

Regarding the statistical tool to predict a higher risk, the copula theory has been well accepted and used to calculate multivariate return periods of natural hazards. De Michele et al. (2007); Bernardara et al. (2014) wrote extensively on the subject with guidelines on using copulas to predict storm surges. More specifically, Kole et al. (2007) found that the Student's and Gumbel copulas are particularly interesting for risk management applications. Liu and Han (2017) deemed that the Clayton and Gumbel copulas are to be preferred for calculating multivariate joint return periods of natural hazards. Many methods are currently in use when estimating the probability of storm surges from sea states such as numerical models (SWAN or SWASH for example) as well as models based on wave energy. However, a more statistical approach based on bivariate copulas combining wave height and sea elevation are also widely used as they are reliable and computationally inexpensive, as seen in Salvadori and Michele (2007) but Orcel et al. (2020) expanded the method to trivariate copulas, allowing the method to yield the probability of structural failure. As indicated by many sources, we have a large choice of different copulas to link our different deep water conditions (Durante and Sempi, 2010, 2016; Tootoonchi et al., 2022). Among them, the Gumbel-Hougaard Copula is commonly used to link the Still Water Level to the wave height as done by (Wahl et al., 2010; Chini and Stansby, 2006). As mentioned by Orcel et al. (2020), this will lead to the calculation of an "and" return period, yielding the expected mean time between two events where all metrics overreach a certain level (as opposed to a "or" return period where only one metric needs to overreach). However, there are very few research on the assessment of erosion of dyke combining statistical and probability approaches and theoretical and semi-empirical approaches as well. Mehrabani and Chen (2015) worked on a joint probabilistic approach for the assessment of climate change's effect on hydraulic loading. However, the authors constrained themselves to the frame of copula theory, assessing the risk to offshore conditions. That approach has considered neither interaction with a dyke nor propagation of deep water wave, but rather physical erosion criteria to put a threshold metric. In the present study, we used global sensitivity analysis to assess the most important parameters in the framework as the ones that contribute to the most variance of the system in order to provide self-improvement to the framework as well as recommendations to improve the resilience of the dyke. Combining different approaches, sensitivity analysis, a fully functional and modular overtopping framework, and copula theory into a full stack has not been explored before and might provide useful guidance for the practitioner. Most works that laid the foundation for the last EurOtop manual (van der Meer et al., 2018) predict wave behavior up to overtopping but do not go further than this point. The focal point of such study is often led by damages to infrastructures laid behind the dyke so the aforementioned limitations made sense. However, providing this extra step allows quantification of the erosion damages provoked on the dyke itself which is the main focus here as salt marshes do not bear costly infrastructures to protect. Also, erosion damage is often easier to observe and quantify than the overtopping phenomenon which is quick, volatile, and difficult to measure on-site. The second section will describe the data used in the study. The third section will be focused on the methodology of the article, and the most important equations regarding both the physical wave process and the statistical processes. Results are presented in the fourth section followed by discussions on the advantages and shortcomings of the study as well as future potential improvements in the fifth section.

2 Data

The statistical study of coastal events requires relatively large, well-documented, and high-quality datasets. Such historical data is not easy to find even in an area containing a dense network of coastal sensors. As a unified database of all records regarding offshore and coastal characteristics does not exist, we used data coming from different bases which contained the measures of interest with correct time synchronicity. We present the data in this section.

2.1 Bathymetry

We have at our disposal the bathymetry of the dyke up to the deepwater point provided by the SHOM. The survey has a resolution of 3 meters and spans over 6 km. As the distance from the dyke to the ANEMOC point (fig. 1) is greater than 6 km, we use all the available data to calculate the mean slope of the beach in front of the dyke.

2.2 Sea level records

As there is no sensor that recorded the sea level in the immediate vicinity of the dyke, which would be highly sensitive to waves anyway, we had to resort to the nearest gauge that had a large record of measures, which was located in Marseilles's harbor (fig. 1). The data of the gauge is maintained by the SHOM[1] in the REFMAR database which is part of the Global Sea Level Observing System[2] (GLOSS) and provides more than 100 years of hourly water elevation level. The acquisition is done using a permanent GNSS station. The place being located inside a port is protected from sea waves. It is located kilometers away from the actual site but we will use these values as no on-site data is available currently. Sea level being forced by atmospheric, mainly wind, conditions, non-linear effects are to be expected between sites, even when the tide gauges are relatively close. This underlines the importance of using on-site data whenever possible. The other issue would be the desynchronization of the data which is accounted for by our peak value selection method (fig. **??**).

2.3 Significant Wave Height records

In situ data of the significant wave height provided at an hourly rate are difficult to find reliably over a long period of time (decades). This means that we have to resort to data provided by a numerical model. We use the data extracted from the ANEMOC-2[3] database currently maintained by the CEREMA[4], reproducing numerically the sea conditions over a long period of time (from 1980 to 2010). The data is generated using the third generation of the TOMAWAC spectral model which is a part of the TELEMAC-MASCARET software suite. This model is used to interpolate sea states on many points calibrated using the GlobalWave *in situ* data. The significant wave height is estimated by calculating the mean value of the upper third of the recorded waves every hour. Thus, one value is given hourly at each chosen location. We have selected point 3667 (fig. 1) as it is located in front of the dyke and where the water depth is high enough to be considered as offshore (≈ 80 m) as

---

[1]https://data.shom.fr/

[2]https://gloss-sealevel.org/

[3]https://candhis.cerema.fr/

[4]https://www.cerema.fr/fr

the continental shelf has been reached according to bathymetry maps. It should be noted that model data carry an intrinsic uncertainty compared to experimental data, which is bound to decrease the reliability of the study.

2.4 Identifying storm surges and coupling the data sets

The time series data itself is not directly exploitable as the copula that we want to generate is based on the identification of extreme events implying a locally high value of both N and H_0 that we will call here "storms". We use the same protocol as in Kergadallan (2015) which is :

- Search for high peak values H_i on data set A (the significant wave height) with a chosen selection method. We use the block maxima approach here;

- Associate each value H_i with its time of occurrence t_i;

- Define a time window Δt which would be the expected mean duration of a storm;

- For each peak, look for the maximum value N_i of data set B (the sea level for example) during the $[t_i - \Delta t/2; t_i + \Delta t/2]$;

- create the couple (H_i, N_i) as the characteristics for storm i.

It is recommended to search for the peak values on the physically most significant dataset, H in our case. However, we applied the same protocol while searching for the peak values on the N dataset and noticed no difference in the resulting distribution, which is what we are looking for. The choice of the block size is not obvious as a small block size decreases the accuracy of the fit to the limit distibution (GEV), leading to a bias, but a large block size reduces the size of the sample, increasing the variance. The general approach is to consider the duration of the cycles between events (for example, seasonal events should use a block size of one year). In our case, storm surges happen regularly during the year so we used a time window of $\Delta t = 33$ hours, obtained by calculating the average duration of events where H exceeds the height threshold. We use this value as a minimum distance between peaks and as a search window to synchronize data. This value allows us to accurately identify the peaks values.

As a preliminary check, correlation coefficients have been calculated to determine the relationship between the datasets. Pearson's Coefficient gave ≈ 0.6, indicating a strong positive relationship. However, Pearson's coefficient is only applicable for linear correlations, which is unlikely, and is inappropriate to capture outliers influence, making it artificially high. Kendall's and Spearman's coefficients are more appropriate in this case and gave ≈ 0.065 (with a p-value of 0.002) and ≈ 0.095 (with a p-value of 0.003) respectively. These values indicate a weak correlation which indicates the dependency structure might not be captured by the ndices and instead calls for another approach, based on copulas.

3 Methods

3.1 Multivariate statistical theory using copulas

The copula method is a popular approach for estimating return periods of extreme events in hydrology or finance and is commonly used as a tool of risk management as univariate statistical analysis might not be enough to provide reliable probabilities with correlated variables as stated by Chebana and Ouarda (2011). One key advantage of the copula method over other methods is that it allows more flexible modeling of the dependence structure between variables. Other methods, such as the traditional joint probability method or the design storm method, assume a specific type of dependence structure (e.g. independence or fixed correlation), which may not accurately reflect the true relationship between the variables. In addition, the copula method can provide more accurate estimates of extreme events and their return periods, especially for events with very low probabilities of occurrence. This is because the copula method allows for a more precise estimation of the tail dependence between variables, which is important for accurately estimating extreme events. As we are looking for rather rare events in this study, this represents a considerable advantage. It however appears that the practitioner has a large selection of copulas to choose depending on the nature of the data. The choice of which copula to choose varies from the type of data as well as the physics of the setup and even so we are left with a rather large selection. Merging multiple copulas in order to combine their properties has also been explored by Hu (2006), complicating further the decision process. Wahl et al. (2010) suggested that the Gumbel-Hougaard copula was particularly adapted when combining water level and wave intensity, although they used the time integral of the wave height over a threshold instead of the significant wave height and the region of interest was the North Sea. Orcel et al. (2020) also recommended using the Gumbel-Hougaard or Clayton copulas for coastal waves on the Atlantic shores of France. An application of the Gumbel-Hougaard copula has also been explored on UK shores aiming to study extreme coastal waves by Chini and Stansby (2006). This motivates us to directly use the Gumbel-Hougaard copula as the most adapted choice (eq. 1).

$$F(u,v \,|\, \theta) = \exp\left[-\left[(-\log(u))^\theta + (-\log(v))^\theta\right]^{1/\theta}\right] \tag{1}$$

where u and v are the cumulative distribution functions of the histograms originating from the data sets. The copula parameter θ represents the interdependency of the data.

The value of this copula parameter is important, and can be calculated using a panel of different methods, ie. the Error method (see Appendix B for the equation as written by Capel (2020)) and Maximum-Likelihood method.

Once done, the copula can be calculated using equation 1, attributing a probability of occurrence of any event E with one of the variables having a value smaller or equal to the defined ones, noted $E(H \leq h || N \leq n)$. The logical inverse $E(H > h, N > n)$ can then be obtained by calculating the survival copula C_θ^{-1} defined as :

$$C_\theta^{-1} = C_\theta + u + v - 1 \tag{2}$$

Finally, we can associate each value of C_θ^{-1} to a return period using the formula provided in Salvadori and Michele (2007) :

$$RP_{=} \frac{\mu}{C_\theta^{-1}} \tag{3}$$

where μ is the average interarrival time between two events of interest i.e., the storms. The offshore conditions have been

determined by a couple (N, H), the water level, and the significant wave height respectively, with an associated return period.

160   This gives us the properties of an offshore wave.

3.2 Maximum-Likelihood Method

The principle of the maximum-likelihood method that we use is that we try to maximize the function L in (eq. 4) yielding the

likelihood of generating the observed data for a set value of θ. It essentially means that given a set of data, a high value of L

indicates that the function is highly likely to have been able to generate the data sample.

165   $$L(\theta) = \sum_{i=0}^{n} c_\theta(u(i), v(i)) \tag{4}$$

where c_θ is the copula density, which can be obtained by calculating the derivative of the copula function with respect to its

cumulative density functions in (eq. 5):

$$c_\theta(u, v) = \frac{\partial^2 C_\theta(u, v)}{\partial u \partial v} \tag{5}$$

3.3 Wave theory : from offshore to the critical velocity

170   We are able to link a deep water state to a return period. However, this does not give us any information on the probability of

the occurrence of an event that would provoke erosion. Hence, we need to assess what kind of event provokes erosion using

equations 6 - 11 to calculate the terminal velocity of the flow on the landward slope.

3.3.1 Propagation

The offshore significant wave height can be propagated up to the toe of the dyke. Among the numerous methods, the most

175   convenient one to use is the propagation formula written in equation 6 extracted from Goda (2000) allowing us to calculate the

significant wave height at the toe of the dyke H_{m0}, which is the mean of the third of the highest wave height over a set period

of time, as follows. This metric is important as it is bound to be used for future calculations of the overtopping characteristics.

Note that refraction is neglected in our case :

$$H_{m0} = \begin{cases} K_s H_0 & \text{for } \frac{d}{L_0} > 0.2 \\ \min\left[\beta_0 H_0 + \beta_1 d; \beta_{max} H_0; K_s H_0\right] & \text{for } \frac{d}{L_0} < 0.2 \end{cases} \qquad (6)$$

where H_0 is the offshore wave height. K_s is the shoaling coefficient, d is the water depth at the toe of the dyke and L_0 is the deepwater wavelength. The coefficients β_0, β_1 and β_{max} can be calculated as detailed in Goda (2000)[5] :

3.3.2 Overtopping equations

Once the wave reaches the toe of the dyke, the wave will start interacting with the dyke in what is called the overtopping phase. This phenomenon is divided into 3 steps with equations detailed in van der Meer et al. (2018). We give a brief summary here of the used equations :

- **Run-up** : The wave reaches the dyke and flows up towards the crest. The run-up height reached by 2% of the incoming waves is calculated (eq. 7).

$$RU_{2\%} = \gamma_f \cdot \gamma_\beta \cdot \left(4 - \frac{1.5}{\sqrt{\gamma_b \cdot \xi}}\right) \cdot H_{m0} \qquad (7)$$

where ξ is the Irribarren Number, H_{m0} is the wave height at the toe of the dyke. The γ factors γ_b, γ_f and γ_β yield the contribution of the berm, the roughness and porosity of the seaward slope, and the obliquity of the waves, respectively.

- **Crest flow** : The water flows on the crest up to the landward slope. We calculate the flow velocity (eq. 8) and thickness (eq. 9) at the beginning of the crest using the previously calculated run-up height.

$$v_{A,2\%} = c_{v2\%} \left(g(RU_{2\%} - z_A)\right)^{0.5} \qquad (8)$$

$$h_{A,2\%} = c_{h2\%}(RU_{2\%} - z_A) \qquad (9)$$

With $c_{v2\%}$ and $c_{h2\%}$ arbitrary coefficients that are used as fitting parameters. Z_A is the height of the dyke above the still water level and g the gravitational acceleration. These equations were compiled in van der Meer (2011); van der Meer et al. (2012) from the works led by Shüttrumpf and van Gent (2003) and Lorke et al. (2012).

The flow velocity will then decay along the crest (eq. 10)as a function of distance from the seaward side of the crest (x_c). It is important to note that this formula is only valid for a few meters long crests as the formula becomes less precise for higher values of x_c.

---

[5]This method is convenient and easy to use but can be imprecise, especially if the deepwater steepness is highly irregular and not constantly positive. The results can then be confirmed using numerical simulations using a wave propagator such as Tomawac. Sergent et al. (2015) gave an estimation of the reliability of the simplified Goda modal compared to numerical methods (BEACH and SWAN for instance), they obtained a reasonable concordance for a steepness inferior to 7%, which corresponds to our case study.

$$\frac{v_{2\%}(x_c)}{v_{2\%}(x_c = 0)} = exp(-1.4x_c/L_0) \tag{10}$$

With $L_0 = g \cdot T_0^2$ the deep water wavelength of the incoming waves.

According to van der Meer et al. (2012), the decrease of flow thickness upon reaching the crest is about one third and can be attributed to the change of direction of the flow and stays relatively constant along the crest.

205

- **Landward slope flow** : The water trickles down the landward slope, this is where erosion usually happens. Terminal velocity (eq. 11) is quickly reached on such slopes so we can use this formula directly instead of the landward flow velocity.

$$v_b = \sqrt[3]{\frac{2 \cdot g \cdot h_{b0} \cdot v_{b0} \cdot \sin\beta}{f}} \tag{11}$$

210 where h_{b0} and v_{b0} are the flow thickness and velocity at the entry of the slope, respectively. f is the friction coefficient, which is determined experimentally whenever possible (an estimation can be used instead if experiments are unavailable), g the gravity acceleration and β the slope angle.

These equations rely on a large number of parameters that are detailed in the table below.

Variable Name	Description	Value in (fig. 5)	Variation Interval	Unit	Source
H_{dyke}	Height of the dyke	2.2	$[1.89, 2.47]$	m	*in situ* data
f	Friction coefficient	0.02	$[0.01, 0.03]$	-	EurOtop (2018)
β	Landward slope	30°	$[20^o, 50^o]$	degrees	*in situ* data
α	Seaward slope	30°	$[20^o, 50^o]$	degrees	*in situ* data
γ_f	Influence of roughness and porosity	0.6	$[0.4, 0.8]$	-	EurOtop (2018)
γ_b	Influence of berm	1.0	$[0.75, 10]$	-	EurOtop (2018)
d	Water depth at the toe of the dyke	0.54	$[0.47, 0.82]$	m	*in situ* data
C_{h2}	Arbitrary coefficient of equation 9	0.2	$[0.1, 0.4]$	-	EurOtop (2018)
C_{v2}	Arbitrary coefficient of equation 8	1.4	$[0.7, 2.1]$	-	EurOtop (2018)
θ	Interdependence parameter (copula)	1.6	$[1.45, 1.75]$	-	Numerical Estimator
v_c	Critical erosion velocity	2	$[1, 4]$	m/s	Hughes (2012)
b_0	First coefficient of equation A1	0.028	$[0.028, 0.052]$	-	Goda (2000)
b_1	First coefficient of equation A2	0.52	$[0.52, 0.63]$	-	Goda (2000)

Table 1. Main control parameters in the equation system of the framework with their reference value and their interval of variation for the GSA.

Defining the value of these parameters is not easy and they may carry some amount of uncertainty that needs to be quantified. We propose a sensitivity analysis to resolve this problem.

3.4 Return period of soil erosion

We can now associate a terminal velocity with a set $\mathcal{S}_{vt} = \{(N, H_0), f(N, H_0) = v_t\}$ that is the set of couples (N, H_0) through the function f to a terminal velocity v_t.

By integrating the derivative of the copula with respect to H_0 along the isoline $\mathcal{S}_{vt}$, we can obtain the return period of event $E_{vt} = \{v_t* > v_t\}$ which is any event implying a terminal velocity equal or higher than v_t (see equations 12 to 14).

$$P(v_t^* > v_t) = \iint\limits_{\mathcal{C}} \left(\frac{\partial^2 C_{N,H_0}}{\partial N \partial H_0} \right) dN dH_0 \tag{12}$$

$$P(v_t^* > v_t) = \int\limits_0^\infty \left[\frac{\partial C_{N,H_0}}{\partial H_0} \right]_{\mathcal{S}(H_0)}^\infty dH_0 \tag{13}$$

$$P(v_t^* > v_t) = - \int\limits_0^\infty \left(\frac{\partial C_{N,H_0}}{\partial H_0}(\mathcal{S}(H_0), H_0) \right) dH_0 \tag{14}$$

Where C is the surface of integration, which is the area above the velocity curve and $S(H_0)$ the velocity curve. This means that we can calculate the return period associated with a certain terminal velocity threshold for a defined dyke by fixing the parameters in Table 1. We give reference values to these parameters. They are obtained either experimentally from *in situ* data or extracted from the literature when observations are unavailable. The details of the values are explained in subsection 3.5.1.

3.5 Sensitivity analysis through the Quasi-Monte-Carlo process

3.5.1 Uncertainty Parameters

The showcased system is indeed able to provide return periods associated with events leading to erosion or any dangerous event defined as a criteria on flow velocity. However, added to the deep water conditions used to generate the copula, are the characteristics associated with the dyke as well as many empirical parameters used to fit the laws allowing the calculations leading to the landward terminal velocity of the dyke. All of these parameters carry an intrinsic amount of uncertainty which has a non-negligible impact on the results. This calls for an accurate quantification of the whole potential range of variation of each parameter. Global sensitivity analysis through the computation of global sensitivity indices will be our tool of choice. A combination of the 1-st order and total effect sensitivity indices (eqs. 17-18) is a principled and classical approach that encapsulates a useful enough amount of information on the variation of the system's characteristics.

We estimate the value of the indices using the Saltelli estimator defined in Saltelli et al. (2008). The number of dimensions being high, we accelerate the convergence of the estimator using a pseudo-random sampler, in our case the Sobol sequence,

240 which generates a low discrepancy sample of points. The resulting distribution of the parameters is thus uniform, which is
standard for the Monte-Carlo method. The performance comparison of the Monte-Carlo process against the improved Quasi-
Monte-Carlo estimations has been extensively discussed, noticeably in Sobol' (1990, 1998); Sobol´ and Kucherenko (2005);
Acworth et al. (1998). The improvement in performance is unanimously in favor of the Quasi-Monte-Carlo Method.

The first step is to define the parameters used in equations (1 - 11) that we are going to consider as relevant sources of
245 uncertainty. They are compiled into Table 1 where we associate a potential range of variation that is deemed as reasonable with
its source. Each parameter is further described in its associated description below. We also provide a brief description of the
parameters as well as the estimation technique.

- **The height of the dyke** H_{dyke} is defined as the vertical distance between the still water level in a calm sea condition
  and the culminating point of the dyke. Using *in situ* data from a Litto3D bathymetry map, we managed to obtain the
250 distribution of the dyke height. We use the mean of the heights as the reference value (tab. 1) and give for sensitivity
  analysis an interval of variation that is approximated by the standard deviation. The same procedure is done for the
  geometrical parameters α, β and d.

- **The friction coefficient** f yields the resistance of contact between two materials, in our case between the landward slope
  of the dyke and water. A higher coefficient brings a slower flow velocity but also more shear stress. Different values can
255 be used here. It is generally considered that for smooth surfaces and vegetation, a value close to 0.02 can be used. We
  assume that is it possible to use such value for small rocks with a diameter of approximately 20 cm, which is what is
  currently implemented on the Quenin dyke.

- **The landward slope** β is defined from the end of the crest which is considered as flat. The steeper is the slope, the
  higher is the terminal velocity. It should be noted that a combination of high crest velocity and steep landward slope can
260 provoke a flow separation at the end of the crest followed by an impact on the slope, resulting in added normal stresses.
  This behavior may be significant and has been explored by Ponsioen et al. (2011).

- **The seaward slope** α is defined as the mean slope from the toe of the dyke to the beginning of the crest, assuming that
  the crest is flat. Its value is important as the behavior of the up-rushing wave may change drastically for different values
  of α.

265 - **The influence of roughness and porosity** on the seaward slope γ_f is a factor with a value ranging from 0 to 1 scaling
  how much the run-up will be attenuated thanks to the slope surface characteristics (1 means no influence). This is difficult
  to estimate as it relies on *in situ* experiments. Evaluating this parameter is not easy. Hence, we chose a relatively large
  range of variation around the reference value as the rocks on the slope are expected to have an influence of the same
  order of magnitude as other structures described in the EurOtop.

270 - **The influence of the berm** γ_b with a value between 0 and 1 indicates the attenuation of the wave due to the presence
  of a berm. This value can be estimated using the geometry of the dyke if it is simple. It is more uncertain for a more

complicated geometry. We calculate this factor using equations given in the EurOtop. The dyke is heterogeneous through its length and its geometry is more complicated than what is used for the calculation as it is a natural berm. Thus we gave it some variability deciding that it could not result in more than 25% water height reduction, which is already dramatic.

– **The depth at the toe of the dyke** b is calculated *in situ* using the Litto3D map as previously cited. Its value is registered for every transversal cross-section of the dyke.

– **The scaling coefficients of the input crest velocity and thickness** C_{h2} and C_{v2}, respectively, are scaling factors on the equations calculating the velocity and thickness of the flow at the beginning of the crest from the run-up. The range is estimated as a variation of $+/-50\%$ from their suggested values in the EurOtop (2018).

– **The correlation parameter** θ determines the intensity of the correlation between the datasets. The results obtained from the MLE estimator suggests that a small plateau is located around the maximum value, so a 10% variation interval is a reasonable assumption here.

3.5.2 Sobol indices

If we provide our framework inputs that are uncertain, it should be expected that the uncertainty will be carried through the system up to the outputs. We rely on sensitivity analysis to quantify such uncertainty by comparing the influence of each parameter on the variation of the outputs relative to their respective range of variation. Since there may be a lot of interaction between parameters and we need to assess the influence of the parameters over their whole range of variation, we use global sensitivity analysis.

Let $Y = f(X_1, ..., X_n)$ be a function of the X_i parameters with $i = 1, ..., n$. The uncertainty of the parameters X_i will carry over the uncertainty of the output Y. Therefore, it would be necessary to estimate the impact of parameters on the output Y.

In order to quantify the influence of a single parameter X_i on a complex system, a good starting point can be to fix this parameter to a defined value x_i. Logically, freezing a parameter, which is a potential source of variation, should reduce the variance $V(Y)$ of the output Y. Hence, a small value of variance $V_{X_{\sim i}}(Y|X_i = x_i)$ would imply a high influence of the parameter X_i. We can globalize the approach by calculating the average value of the variance over all valid values of x_i, preventing the dependence on x_i. This is written as :

$$E_{X_i}(V_{X_{\sim i}}(Y|X_i = x_i)) < V(Y) \tag{15}$$

The following relation is also useful in our case :

$$E_{X_i}(V_{X_{\sim i}}(Y|X_i = x_i)) + V_{X_i}(E_{X_{\sim i}}(Y|X_i = x_i)) = V(Y) \tag{16}$$

The conditional variance $V_{X_i}(E_{X_{\sim i}}(Y|X_i = x_i))$ is called the first-order effect of X_i on Y. We can then use the sensitivity measure called the sensitivity index or Sobol index (see Sobol (2001)) defined as :

$$S_i = \frac{V_{X_i}(E_{X_{\sim i}}(Y|X_i = x_i))}{V(Y)} \tag{17}$$

This gives the proportion of contribution of the parameter X_i alone on the total variance of the output Y relatively to the other parameters $X_{\sim i}$. The main drawback of this measure is that the interaction of the parameters between themselves is not taken into account. These measures are contained in higher-order indices. However, this may become quite time-consuming and impractical if the number of parameters is high as the total number of Sobol indices that could be calculated grows as $n!$ with n the number of parameters.

The Total Effect Sobol' Index, which measures the influence of a parameter i on the variance as well as its interaction with every other parameter is calculated following the same method but instead of freezing parameter i, we freeze every other parameter $j \neq i$ (eq. 18).

$$S_{Ti} = 1 - \frac{V_{X_i}(E_{X_{\sim i}}(Y|X_i))}{V(Y)} = \frac{E_{X_i}(V_{X_{\sim i}}(Y|X_i))}{V(Y)} \tag{18}$$

Although concise, the equations 17-18 are difficult to calculate analytically. We circumvent the problem by using the method developed by Sobol (2001) and further improved by Saltelli et al. (2008). The protocol can be summarized as follows (fig. 2) :

– Define the input parameter space and the model output function.

– Generate a set of samples using Latin hypercube sampling (LHS) or another quasi-random sampling method (we used Sobol' sequence in our case).

– Compute the model output for each set of input parameters.

– Partition the output variance into components due to individual input variables and their interactions using an ANOVA-based decomposition.

– Calculate the first-order and total-effect Sobol indices, which measure the contribution of individual input variables and their interactions to the output variance, respectively.

The procedure can be summarized as a dual process of using statistics, copula theory to generate a copula associating return periods to a couple (N,H) of deepwater metrics on one side and calculating the interaction of the same couple (N,H) with the dyke to calculate the landward slope velocity on the other side. This whole chain can then be inputted into a global sensitivity analysis method (fig. 2).
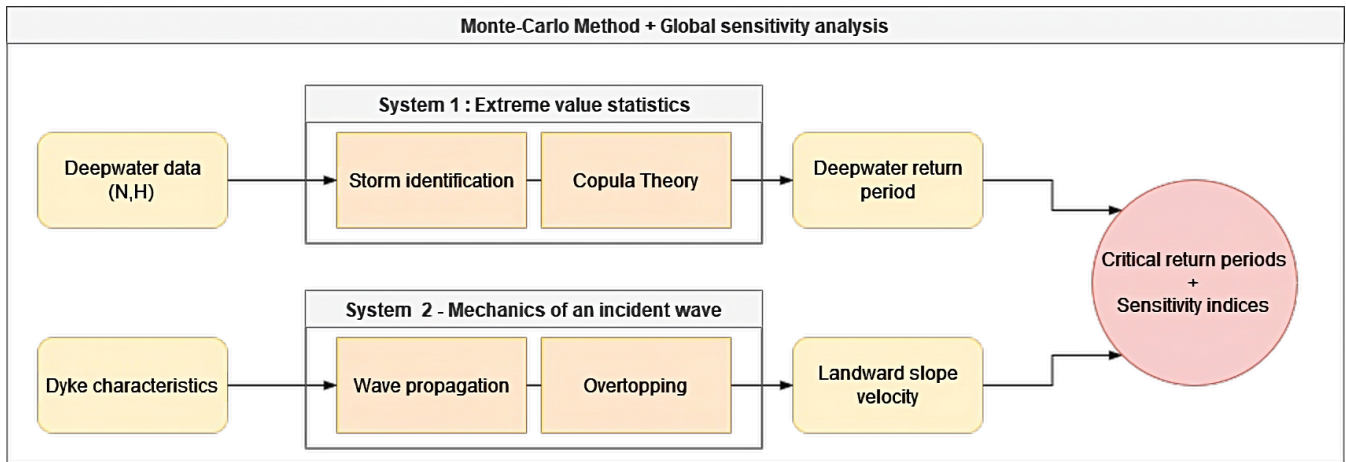
Figure 2. Diagram highlighting the main steps of the process as well as involved methods

4 Results

4.1 Return Periods Copula

We start by compiling the selected storm surge events into a histogram, giving the univariate probability densities of both datasets. However, since we only work with about 20 years of hourly data, we need to fit the cumulative histogram in order to create a cumulative distribution function that allows us to extrapolate to rarer events. We use the Generalized Extreme Value distribution which is used for the estimation of tail risks and is currently applied in hydrology for rainfalls and river discharges in the context of extreme events as in Muraleedharan et al. (2011).

This means that the events can then be sorted into a histogram for us to observe their respective univariate distributions. In this case, the sample limits us to events that can happen up to once every 20 years since we have no data covering a larger period. Thus, we can can obtain information about more extreme events by extrapolating the data using a fitted distribution on each individual sample. Using the block maxima event selection, the Fisher-Tipett-Gnedenko Theorem indicates that extreme values selected this way asymptotically follow the Generalized Extreme Value distribution (GEV) (eq. **??**).

As a sanity check, we decided to compare it to other similar distribution that can be used to model hydrological events using a using a Kolmogorov-Smirnov test, which gave :

Name of the distribution	KS-score	P-value
Generalized Extreme Value	0.023	0.63
Weibull	0.05	0.005
Gamma	0.04	0.07
Log-normal	0.024	0.57

Table 2. The different tested distributions with their respective KS-score and p-value

The general approach consists in choosing the distribution displaying the lowest KS-score with the highest p-value when
340   possible, which in our case is the Generalized Extreme Value distribution. Thus we will use it for the rest of the study. The Gumbel law could have also been chosen as it is encapsulated by the GEV it would have brought very similar results. We stick to the GEV as it is the more general case and the theoretical approach.

$$[H]F(x) = \exp(t(x)) \qquad \text{with} \qquad t = \begin{cases} \left(1 + \xi\left(\frac{x-\mu}{\sigma}\right)\right)^{-1/\xi} & \text{if } \xi \neq 0 \\ \exp\left(-\left(\frac{x-\mu}{\sigma}\right)\right) & \text{if } \xi = 0 \end{cases} \tag{19}$$

with (μ, σ, ξ) the location, scale, and shape factor, respectively. The results are displayed in Fig. 3. The laws are fitted using
345   the maximum-likelihood method. The fit gives a R^2 score higher than 0.999 for both data sets. Hence, we consider the fit almost perfect and it will not be accounted for during future calculations of uncertainty as it is considered insignificant compared to other sources.
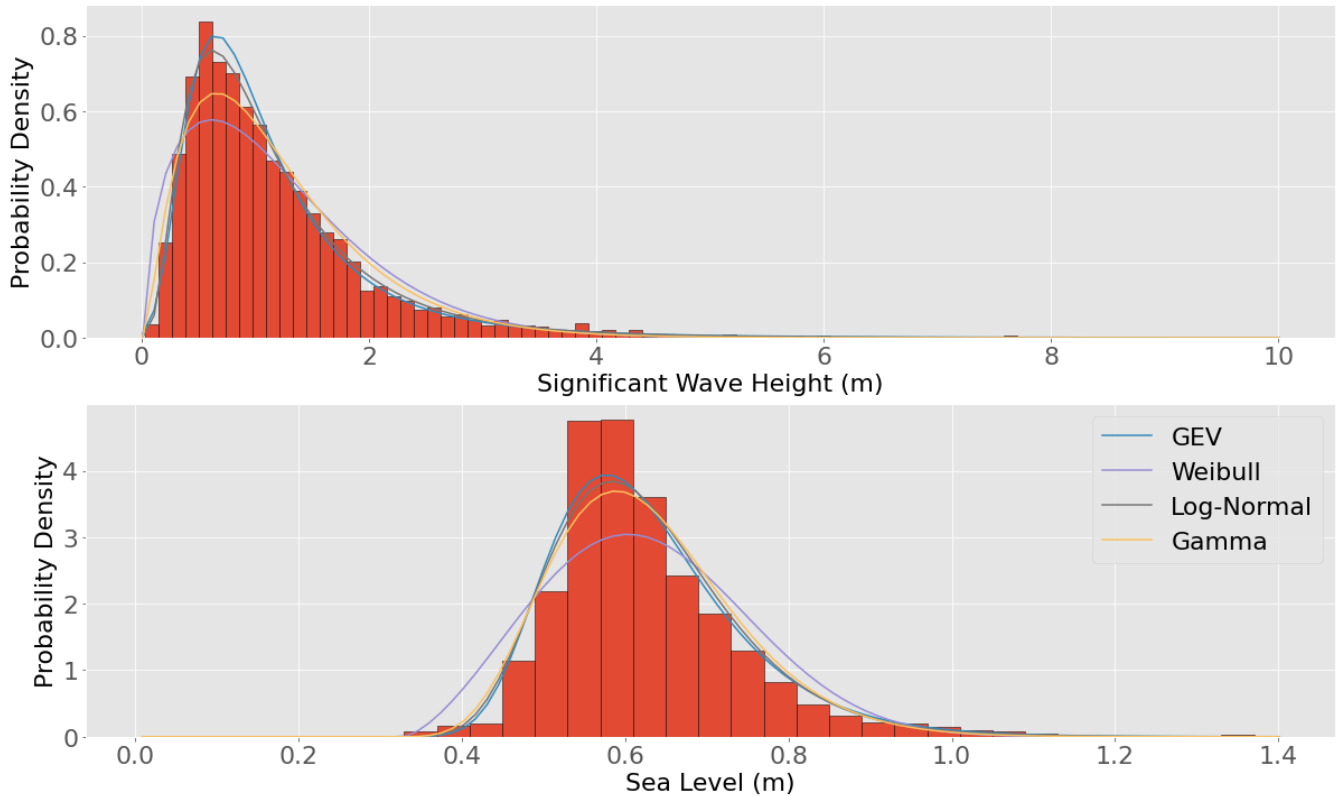
Figure 3. Cumulative Distribution Functions of the offshore significant wave height (a) and the still water level (b) displayed in a histogram. They are fitted to different distributions. Most of them are very similar.

We will then compute the derivative of the copula in (eq. 1) and maximize the value of $L(\theta)$ from (eq. 4).

The interdependence parameter can take values in the interval $[1, +\infty[$, where 1 is the independent copula and $+\infty$ means absolute correlation. A value of 1.6 means that there is a moderate correlation between the two distributions. This can be seen visually in fig. 4 as the contour lines form an L-shape, indicating the values are strongly linked. Hence, we can generate the copula using equation 1. The cumulative distribution function yields the probability of a value laying under a threshold. Hence, we use equation 2 to inverse the copula and obtain the survival copula (fig. 4). This allows us to evaluate the return period of any event E so that $E(N \leq x || H_0 \leq y)$ using (eq. 1-3).
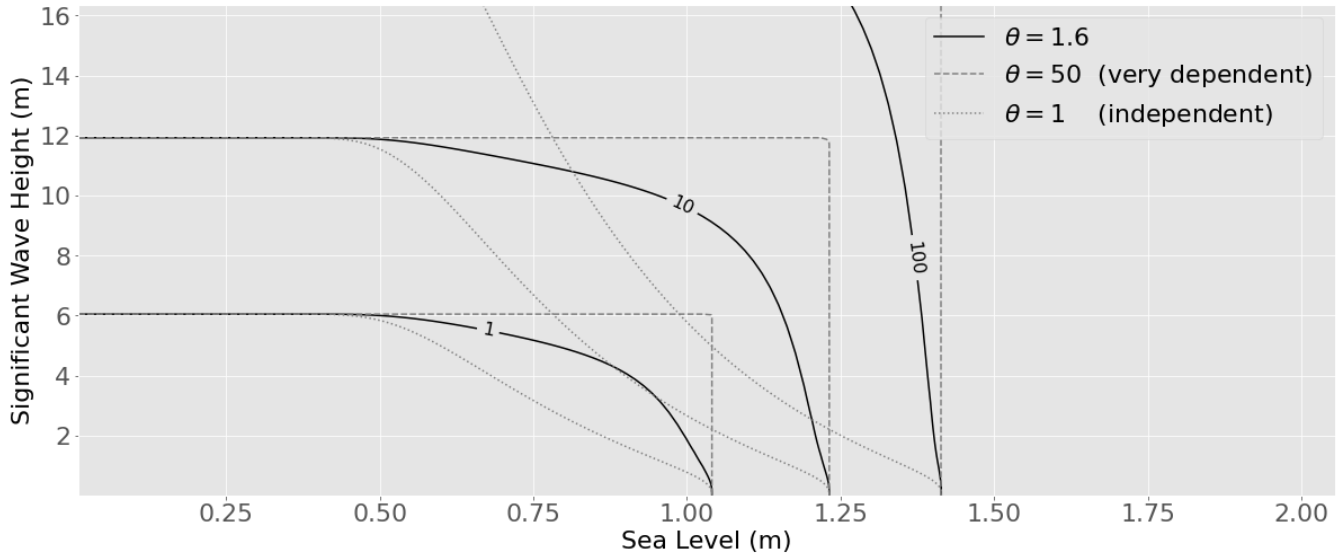
Figure 4. Return period (in years on the contour lines) of an event composed of a couple (N, H_0) or with a higher value of N or H_0, noted as $RP(E(N > x || H_0 > y))$ with the interdependence factor having a value of $\theta \approx 1.6$ (full line). The independent copula (dotted lines) and the high-dependence copula (dashed lines) are also displayed for reference.

The contour lines of the copula in (fig. 4) show that the data are coupled to some degree. Indeed, since the data are correlated, a high value of the water level N and the significant wave height H should be more probable than if the data were uncorrelated, thus decreasing the return period and driving the contour lines toward the smaller values.

4.2 Computing the terminal velocity

We use the terminal velocity on the landward slope v_t as a criterion of erosion. Meaning that damage starts to occur when $v_t > v_c$ where v_c is the critical velocity which has to be determined using the literature. Using (eqs. 6 - 11), we can calculate it from any couple (N, H_0) of offshore water level and significant wave height, given that the mean slope of the bathymetry is known. The results are shown in Fig. 5.

Unsurprisingly, higher values of both N or H_0 induce higher values of terminal velocities. All values below the "0.0" line (fig. 5) failed to produce overtopping and thus generate a null value while in fact there is no water flowing on the slope.
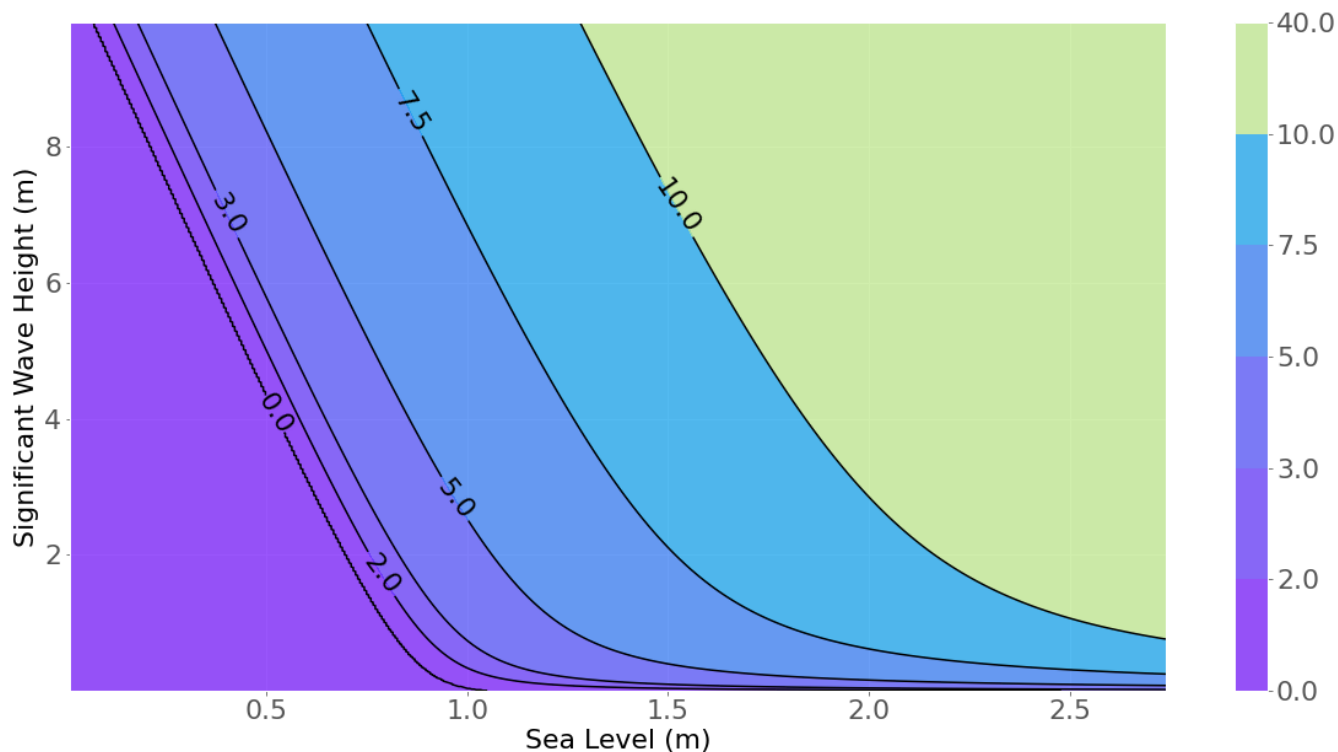
Figure 5. Terminal velocity (in m/s on the contour lines) along the landward slope for any couple (N, H_0). Higher Sea level and Significant wave height bring higher terminal velocity.

365   Typically, we observe that the Quenin dyke's landward slope is covered by rubble mounds which have an average diameter of 20 cm. Applying Peterka's formula (Peterka, 1958) (eq. 20) which is used by the U.S. Bureau of Reclamation, we can obtain the critical velocity of erosion on the dyke.

$$v^* = \sqrt{d_{50}/0.043} \tag{20}$$

where v^* is the critical erosion velocity and d_{50} is the median block parameter. For blocks with a diameter of 20 cm, we
370   obtain a critical erosion velocity of approximately 2 m/s. Our calculations estimate that such flow velocity will occur on average once every 5.86 years. This gives a higher value than what is reported by the Salins du Midi company, currently exploiting the dyke. The company reports significant damage that needs to be repaired approximately once every two years. This has been confirmed by its archives. This gap can be caused by uncertainty on the parameters which will be further estimated via sensitivity analysis.

4.3 Sensitivity indices

After generating a sample of parameter values, each set is computed through the framework, giving an associated return period from which we calculate the global sensitivity indices of both 1-st order and total effect (fig. 6).
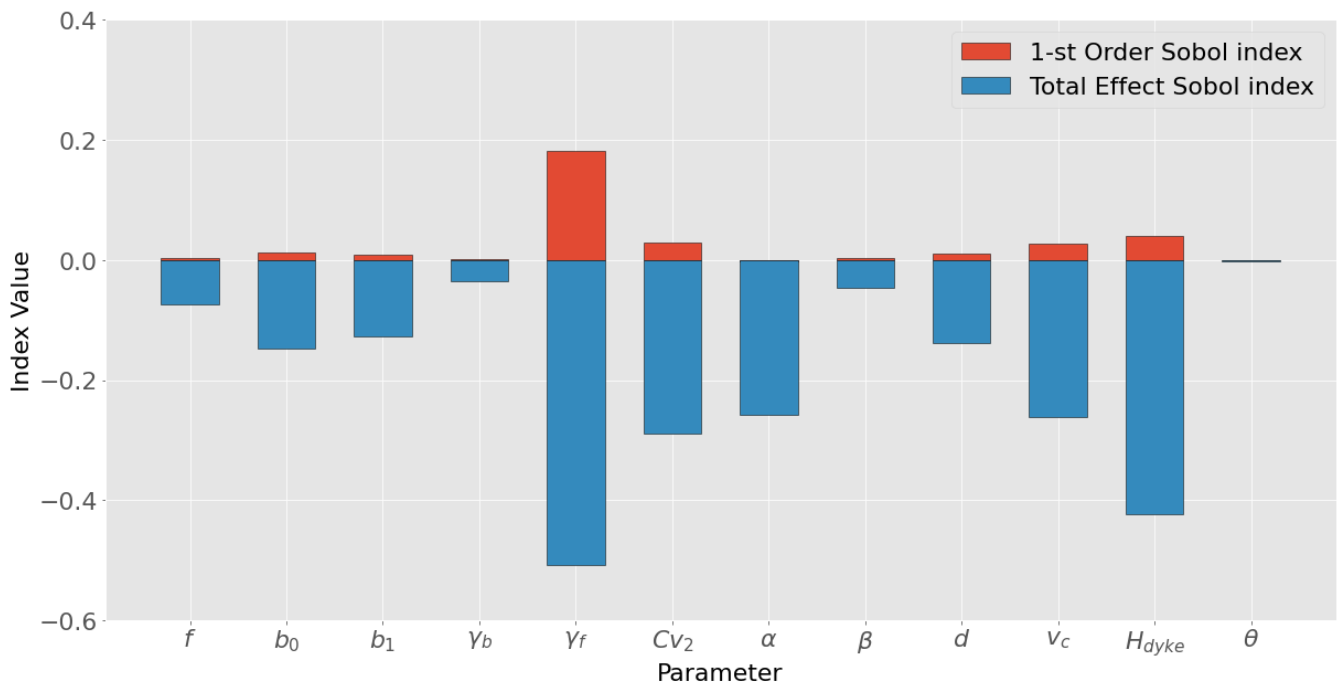
Figure 6. Value of the 1st-order sensitivity (in red) and total effect (in blue) indices for each tested parameter.

A few observations can be made about the results. It appears that there is some correlation between the 1-st order Sobol' index and the Total Effect index. This is not surprising as the Total Effect index encapsulates all orders, including the 1-st order. Then, the considered parameters contribute very differently to the uncertainty of the system. It is essential to remind that high contribution to uncertainty can mean that either that the parameter is very influential or that it is very uncertain (or both). We will focus on the most important parameters here :

– γ_f : This parameter intervenes at the beginning of the overtopping process and thus should present a high degree of interactivity with other parameters, which explains the very high Total Effect Index value. The parameter is undoubtedly very influential since it is a direct coefficient of the overtopping wave height. However, this parameter is very difficult to assess experimentally and we had to rely on reference values for the variation interval. This means that a part of the uncertainty can be explained by a large range of variation defined in the bound of the Global Sensitivity Analysis. This result is corroborated by B.P. et al. (2019) where they proceed similarly and find that the majority of the uncertainty is held by the overtopping process.

- H_{dyke} : The dyke height is one of the most important parameters considered when designing a dyke so observing high Sobol' indices values is not a surprise. Furthermore, the *in situ* showed that the dyke was not homogeneous with height varying between 1.7m and 2.5m. This could be a problem as it reveals the presence of weak points on the dyke where damage could occur, showing the limit of working with reference values. Hence, improving the dyke by making it more homogeneous could reduce the uncertainty of the system.

- V_c : The critical velocity is an important parameter that is heavily studied as one of the main metrics used to quantify erosional damage in the literature (e.g. Hughes and Nadal (2008)). The relative variation interval is also quite large around the reference value (from -50% to $+100\%$) so high sensitivity indices are expected.

These results show the importance of good characterization of the physical parameters of the dyke through experiments in order to reduce the intervals of variations, thus the uncertainty. It also underlines the homogeneity of dyke construction as one of the main concerns of future dyke designs. It finally appears that all processes seem to contribute to the global uncertainty of the system, only the statistical part seems to be insignificant.

4.4 Return periods distribution

Launching such a high number of calculations allows us to compile the return periods into a histogram to evaluate the probability of the return periods taking into account uncertainties. The results are compiled in Fig. 7.
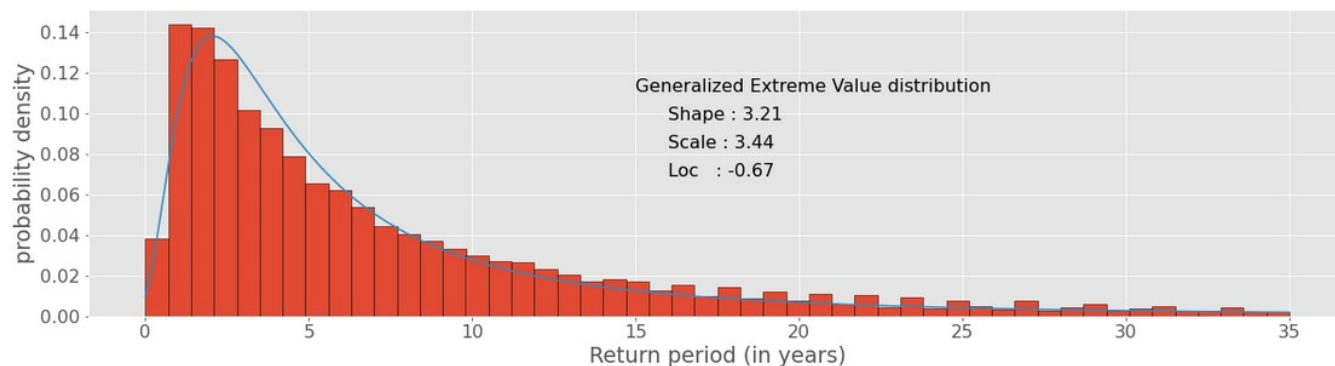
Figure 7. Distribution of the return periods of an event able to provoke some amount of erosion to landward slope at the dyke with random variation of the parameters in Table 1 according to their respective range of variation. The distribution is determined by three parameters : the localization is the beginning of the distribution at $y = 0$, the scale determines how the distribution stretches vertically and the shape controls the skewness of the distribution or how steep the decrease is after the initial peak.

The results show that the distribution can be well-fitted using a Generalized Extreme Value distribution which is right-skewed with a peak around the two years value and a long tail in the upper range of the return periods. The choice of the GEV is motivated by its common use to model extreme events such as floods, winds, and erosion Morrisson and Smith (2002); Chen et al. (2019). Furthermore, the root mean square error was lower on this fit than with other tested distribution such as the

Lognormal or Pareto distribution. The mean value is close to ten years. This is high compared to what is expected from actual

410 *in situ* records. However, the distribution is skewed. The median is of approximately 5 years, which is closer to the records.

The peak value is more representative than the mean as many of the extreme geometries represent weak points that are subject to the frequent erosion that are observed. Historical data gathered from the company monitoring the dyke seem to be in accordance with the choice of the peak value as the representative metrics of the distribution.

5   Discussions

5.1   Results Validation

In order to make sure that the estimation of the sensitivity indices is accurate we need to ensure that the convergence of the estimator has been reached. We will do this by plotting the values of the indices and incrementally increasing the amount of points generated by the Sobol' sequence, this is called a validation curve. Note that the amount of plotting points is limited because the Sobol' sequence, being a non independent sample, is only valid for 2^n points. The results are displayed in (fig. 8).
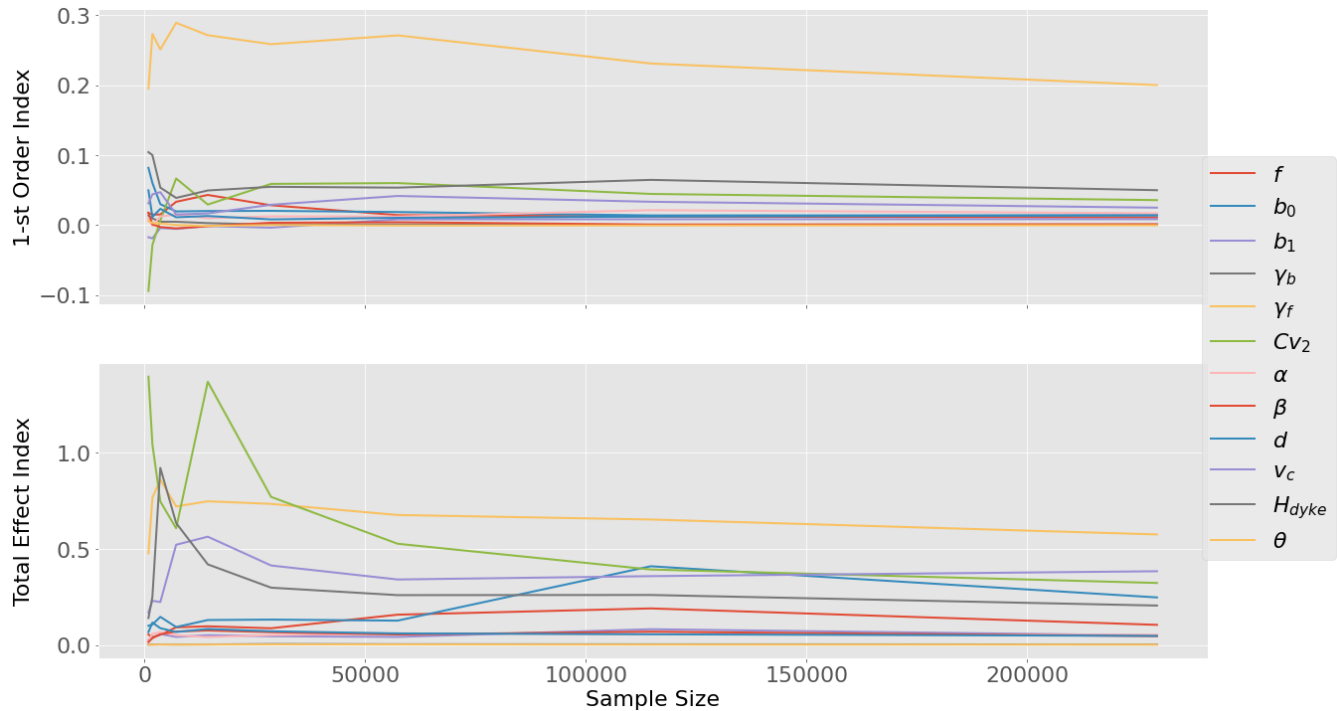
Figure 8. Evolution of the values of the 1-st order sensitiviy index (a) and total effect sensitivity index (b) with sample size.

420   Convergence has evidently been reached. It seems that we can safely use ≈ 125000 points which in our case is still fairly low as the computation of the terminal velocity is pretty fast. However, should the computation time increase by changing the methods of calculation, this could become a problem which would require more intensive optimizations.

5.2   Good practices and dyke improvements

Results from the Global Sensitivity Analysis give indications on how the dyke could be reinforced in order to increase the most the return periods. The recommendation would be to act upon the most significant parameters of the analysis, meaning the ones which yield the highest values of Sobol' indices. This indicates that the geometrical features of the dyke, the crest height as well as the slopes, should be acted upon first whenever possible. Elevating the dyke or decreasing its seaward steepness should bring good results while altering the erosion properties of the landward slope does not look so promising. This focus on the geometrical features of the dyke is supported by Sibley et al. (2017). Generally, the recommendations of the USCE seem to focus mainly on geometrical features and secondly on erosion resistance when considering the design of levees. Approaching the problem using Sobol' indices in this particular use case had not been done before and seems to provide similar results, confirming the value of the method. The recommendations stated here do not include however an analysis of cost-effectiveness which should be one of the next milestones of the work that is presented here.

5.3   Limits of the study

The framework provides a rather complete approach but obviously suffers some limitations. Some of them are inherent to the system itself while others call for future improvements. Our main focus was to obtain an assessment of the risk of erosion on the landward slope of the dyke. Coastal protection is nonetheless submitted to many other damages such as erosion in other locations like the crest of the seaward slope. A more general criterion of security such as "any damage to the dyke" would require to broaden the calculations to take all possible damages into account. We have also limited our criteria of interest as a condition of whether or not the critical velocity has been overreached on the landward slope. The possibility of a breach or the amount of actual amount of eroded material is therefore not quantified. For practical reasons, we calculated return periods on an averaged profile of the dyke which as stated by the global sensitivity analysis can lead to a return period different from the local profile. A location-wise study could bring reduced uncertainty and bring more relevant results. The data sources used to make our analysis are incomplete, located in far away places or generated using numerical models. It is necessary to use *in situ* data extracted from experimental devices in order to improve the reliability of the study. Moreover, the study uses long-term data but the impacts of climate change, implying an elevation of the water level as well as changes in the characteristics of storm surges such as intensity, duration or frequency. Integrating these effects should be done in the future in order to improve long term studies. This problem is especially important for more resilient dykes dealing with higher return periods.

6   Conclusion

We have been able to build a complete automated framework allowing the user to estimate the expected return periods of events leading to erosion on the rear side of the earthen dyke submitted to wave overtopping, assuming the correctly assessed ranges of variation the parameters are provided. The framework itself needs firstly meteocean data in order to create a reliable

copula from wave and water level data, then a description of wave propagation to the toe of dyke, and finally reliable laws representing wave overtopping process, run-off on the crest then on the landward slope and bottom erosion.

455   The return period from which erosion on the Quenin dyke located in Salin-de-Giraud starts is firstly estimated from reference parameters. This first estimate is equal to six years which is significantly higher than the value of two years written in reports from the operating company. The framework is then able to take the parameters' uncertainty into account which provides a Generalized Extreme Value distribution of return periods which is right-skewed with a peak around the two years value and a long tail in the upper range of the return periods. This result shows that a statistical study is necessary to determine

460   a return period of damages in accordance with observed damages. Damages on a long dyke are not observed on an average profile but on the weakest profile. That is why the peak of the statistical analysis is more representative than the first estimate based on average parameters. Sensitivity analysis is implemented into the framework and classifies the dyke's parameters in terms of carried uncertainty. No clear trend can be observed for a specific category of parameter that would carry a significant part of the global uncertainty. However, the protocol allows us to clearly distinguish which parameters should be closely

465   considered and which ones can be ignored. The results underline the importance of characterizing the dyke using experiments and simulations in order to reduce the parameters range of variation as much as possible. All processed contribute significantly to the uncertainty of the system, excluding the statistical treatment. This study case is indeed very specific with a very low return period for damages and large variations of the dyke crest. For any other dyke, the framework is applicable by providing the appropriate input values.

470   Finally, the results can be provided relatively quickly without an enormous amount of computing power. They can be validated indeed using only a small set of points for the Quasi-Monte-Carlo process (around fifteen thousand points at most).

Code and data availability. Freely available on demand to the corresponding author

Author contributions. C. Lutringer - Conceptualization, Methodology, Software, Investigation, Writing - Original Draft, Data Curation, Visualization

475   A. Poupardin - Supervision, Writing - Review and Editing, Methodology, Resources

P. Sergent - Conceptualization, Methodology, Validation, Surveilance, Project Administration, Funding acquisition

A. Bennabi - Conceptualization, Supervision, Project Administration

J. Jeong - Supervision, Writing - Review and Editing, Resources, Funding acquisition, Project Administration

Competing interests. The authors declare that they have no conflict of interest

480 Acknowledgements

We hereby thank the Salins du Midi company for financially supporting the work and especially Pierre-Henri Trapy for providing useful information on the site, guidance as well as access to the company's archives.

References

Acworth, P., Broadie, M., and Glasserman, P.: A Comparison of Some Monte Carlo and Quasi Monte Carlo Techniques for Option Pricing, Springer New York, 1998.

Bergeijk, V. V., Warmink, J., van Gent, M., and Hulscher, S.: An analytical model of wave overtopping flow velocities on dike crests and landward slopes, Coastal Engineering, 2019.

Bernardara, P., Mazas, F., Kergadallan, X., and Hamm, L.: A two-step framework for over-threshold modelling of environmental extremes, Natural Hazards and Earth Systems Sciences, 14, 635–647, 2014.

B.P., G., Y., L., A., F., J., H., and C., M.: Uncertainty and sensitivity analysis of a coastal flood risk modelling chain, EVAN 2019, 2019.

Capel, A.: Wave run-up and overtopping reduction by block revetments with enhanced roughness, Coastal Engineering, 104, 76–92, 2020.

Chebana, F. and Ouarda, T.: Multivariate quantiles in hydrological frequency analysis, Environmetrics, 22, 63–78, 2011.

Chen, B., Zhang, K., Wang, L., Jiang, S., and Liu, G.: Generalized Extreme Value-Pareto Distribution Function and Its Applications in Ocean Engineering, China Ocean ENgineering, 2019.

Chini, N. and Stansby, P.: Extreme values of coastal wave overtopping accounting for climate change and sea level rise, Coastal Engineering, 65, 27–37, 2006.

De Michele, C., Salvadori, G., Passoni, G., and Vezzoli, R.: A multivariate model of sea storms using copulas, Coastal Engineering, 54, 734–751, 2007.

Durante, F. and Sempi, C.: Copula Theory: An Introduction, Lecture Notes in Statistics, 198, 3–31, 2010.

Durante, F. and Sempi, C.: Principles of Copula Theory, CRC Press, 2016.

Goda, Y.: Random Seas and Design of Maritime Structures, vol. 15, World Scientific Publishing Co., 2000.

Hu, L.: Dependence patterns across financial markets: a mixed copula approach, Applied Finance Economics, 16, 717–729, 2006.

Hughes, S. and Nadal, N.: Laboratory study of combined wave overtopping and storm surge overflow of a levee, Coastal Engineering, 56, 244–259, 2008.

Hughes, S., C.Thornton, der Meer, J. V., and Scholl, B.: Improvements in describing wave overtopping processes, Coastal Engineering, 2012.

Kergadallan, X.: Estimation des niveaux marins extrêmes avec et sans l'action des vagues le long du littoral métropolitain, 2015.

Kole, E., Koedijk, K., and Verbeek, M.: Selecting copulas for risk management, Journal of Banking and Finance, 31, 2405–2423, 2007.

Li, T., Troch, P., and Rouck, J. D.: Wave overtopping over a sea dike, Journal of Computational Physics, 198, 686–726, 2003.

Liu, S. and Han, J.: Energy efficient stochastic computing with Sobol sequences, Design, Automation & Test in Europe Conference & Exhibition, pp. 650–653, 2017.

Lorke, S., Borschein, A., Schüttrumpf, H., and Pohl, R.: Influence of wind and current on wave run-up and wave overtopping. Final report., FlowDike-D, 2012.

Mehrabani, M. and Chen, H.: Risk Assessment of Wave Overtopping of Sea Dykes Due to Changing Environments, Conference on Flood Risk Assessment, 2015.

Morrisson, J. and Smith, J.: Stochastic modeling of flood peaks using the generalized extreme value distribution, Water Ressources Research, 2002.

Muraleedharan, G., Soares, C. G., and Lucas, C.: Characteristic and Moment Generating Functions of Generalised Extreme Value Distribution (GEV), Sea Level Rise, Coastal Engineering, Shorelines and Tides (Oceanography and Ocean Engineering), 14, 269–276, 2011.

Orcel, O., Sergent, P., and Ropert, F.: Trivariate copula to design coastal structures, Nat. Hazards Earth Syst. Sci., 21, 1–22, 2020.

520 Peterka, A.: Hydraulic design of stilling bassin and energy dissipators, Engineering Monograph, 25, 222, 1958.

Ponsioen, L., Damme, M. V., and Hofland, B.: Relating grass failure on the landside slope to wave overtopping induced excess normal stresses, Coastal Engineering, 14, 269–276, 2011.

Pörtner, H.-O., Roberts, D., Tignor, M., Poloczanska, E., Mintenbeck, K., Alegría, A., Craig, M., Langsdorf, S., Löschke, S., Möller, V., Okem, A., and Rama, B.: Climate Change 2022: Impacts, Adaptation, and Vulnerability. Contribution of Working Group II to the Sixth
525 Assessment Report of the Intergovernmental Panel on Climate Change, Cambridge University Press, 2022.

Saltelli, A., Ratto, M., Terry, A., Campolongo, F., Cariboni, J., Gatelli, D., Saisana, M., and Tarantola, S.: Global Sensitivity Analysis, The Primer, John Wiley and Sons, Ltd, 2008.

Salvadori, G. and Michele, C. D.: On the use of Copulas in Hydrology : Theory and Practice, Journal of Hydrologic Engineering, 12, 2007.

Sergent, P., Prevot, G., Mattarolo, G., Brossard, J., Morel, G., Mar, F., Benoit, M., Ropert, F., Kergadallan, X., Trichet, J., and Mallet, P.:
530 Stratégies d'adaptation des ouvrages de protection marine ou des modes d'occupation du littoral vis-à-vis de la montée du niveau des mers et des océans, Ministère de l'écologie, du développement durable, du transport et du logement, 2015.

Shüttrumpf, H. and van Gent, M.: Wave overtopping at seadikes, Proc. Coastal Structures, pp. 431–443, 2003.

Sibley, H., Vroman, N., and Shewbridge, S.: Quantitative Risk-Informed Design of Levees, Geo-Risk, 2017.

Sobol', I.: Quasi-Monte Carlo methods, Progress in Nuclear Energy, 24, 55–61, 1990.

535 Sobol', I.: On quasi-Monte Carlo integrations, Mathematics and Computers in Simulation, 47, 103–112, 1998.

Sobol, I.: Global sensitivity indices for nonlinear mathematical models and their Monte Carlo estimates, Mathematics and Computers in Simulation, 55, 271–280, 2001.

Sobol´, I. and Kucherenko, S.: On global sensitivity analysis of quasi-Monte Carlo algorithms, Monte Carlo Methods and Applications, 11, 83–92, 2005.

540 Tootoonchi, F., Sadegh, M., Haerter, J., Raty, O., Grabs, T., and Teutschbein, C.: Copulas for hydroclimatic analysis: A practice-oriented overview, WIREs Water, 9, 2022.

van der Meer, J.: The Wave Run-up Simulator. Idea, necessity, theoretical background and design, Van der Meer Consulting Report vdm11355, 2011.

van der Meer, J., Provoost, Y., and Steendam, G.: The wave run-up simulator, theory and first pilot test, Proc. ICCE, 2012.

545 van der Meer, J., Allsop, N., Bruce, T., de Rouck, J., Kortenhaus, A., Pullen, T., Schüttrumpf, H., Troch, P., and Zanuttigh, B.: EurOtop. Manual on wave overtopping of sea defences and related structures. An overtopping manual largely based on European research, but for worldwide application, www.overtopping-manual.com, 2018.

Wahl, T., Jensen, J., and Mudersbach, C.: A multivariate statistical model for advanced storm surge analyses in the North Sea, Proceedings of 32rd International Conference on Coastal Engineering, Shanghai, China, 2010.

550 **Appendix A: Propagation equations from Goda (2000)**

$$\beta_0 = b_0 \cdot \left(\frac{H_0}{L_0}\right)^{-0.38} * e^{20 \cdot m^{1.5}} \tag{A1}$$

$$\beta_1 = b_1 \cdot e^{4.2 \cdot \tan \theta_a} \tag{A2}$$

$$\beta_{\max} = \max[0.92, 0.32 \cdot (H_0/L_0)^{0.29} \cdot e^{2.4 \cdot \tan \theta_a} \tag{A3}$$

with m the average steepness of the seabed between the offshore point and the toe of the dyke, θ_a the angle of attack of
the oblique waves and L_0 the deep water wavelength. b_0 and b_1 are coefficient determined empirically from Goda (2000) who
gives their values of 0.028 and 0.052, respectively.